Journal Syifa Sciences and Clinical Research (JSSCR)
Volume 6 Number 2, 2026
Journal Homepage: http://ejurnal.unga.ac.id/index.php/jsscr, E-ISSN: 2656-9612 P-ISSN:2656-8187
DOI: https://doi.org/10.37311/jsscr.v8i2.37713

In Silico Evaluation of Goji Berry (*Lycium barbarum*) Bioactive Compounds Targeting BRAF V600E in Melanoma

Collin Angelicha[1*], Azmi Rahmadani[2], Adinda Dwi Fajriati[3], Taghsyana Binurih[4]

[1,2,3,4] *Department of Pharmaceutical Chemistry, Faculty of Pharmacy, Universitas Islam Sultan Agung, Semarang, Indonesia*

** Corresponding author. Email: collinangelicha2004@gmail.com*

ABSTRACT

Melanoma is the most aggressive form of skin cancer and is associated with high mortality, primarily due to aberrant activation of the mitogen-activated protein kinase (MAPK) pathway driven by mutations in the BRAF gene, particularly BRAF V600E. BRAF inhibitors such as vemurafenib have been used in the treatment of BRAF-mutant melanoma; however, their long-term clinical efficacy is often limited by acquired resistance and tumor adaptive mechanisms. Therefore, the exploration of natural product–based adjuvant candidates remains relevant to support melanoma therapy. This study aimed to evaluate the potential of bioactive compounds from goji berry (*Lycium barbarum*) as anti-melanoma candidates through an *in silico* approach targeting BRAF. Molecular docking was performed using the BRAF–vemurafenib complex structure (PDB ID: 3OG7), and the docking protocol was validated by redocking vemurafenib, yielding an RMSD value of 0.956 Å, which indicated the reliability of the docking procedure. Twelve bioactive compounds from *Lycium barbarum* were docked into the BRAF binding site, and their binding affinities, amino acid residue interactions, drug-likeness, and ADMET profiles were analyzed. The docking results showed that zeaxanthin, myricetin, quercetin, ellagic acid, galangin, kaempferol, and chlorogenic acid exhibited binding affinity values ≤ −8.0 kcal/mol, indicating favorable predicted interactions with BRAF. Among the tested compounds, quercetin showed one of the strongest binding affinities and conserved key amino acid interactions comparable to vemurafenib, whereas galangin demonstrated the most favorable drug-likeness and ADMET profile. These findings indicate two complementary prioritization criteria, in which quercetin is superior in predicted binding interaction, while galangin is superior in pharmacokinetic and drug-likeness suitability. Therefore, quercetin and galangin may serve as promising preliminary candidates for further investigation as BRAF-targeting adjuvant agents in melanoma therapy; however, experimental validation through BRAF kinase inhibition assays and melanoma cell-based studies is required to confirm their biological activity and therapeutic relevance.

Keywords:
Goji berry; *Lycium barbarum*; molecular docking; melanoma; BRAF V600E; Vemurafenib; ADMET; Lipinski's Rule of Five

Received:	*Accepted:*	*Online:*
2026-03-08	*2026-05-06*	*2026-05-13*

1. Introduction

Melanoma is the most aggressive form of skin cancer and the leading cause of skin cancer–related mortality worldwide, despite its lower incidence compared to non-melanoma skin cancers [1]. Its global incidence continues to rise, ranking among the most frequently diagnosed cancers, with approximately 132,000 new cases reported annually, largely associated with increased ultraviolet (UV) exposure [1], [2]. UV radiation contributes to melanomagenesis through DNA damage, oxidative stress, and microenvironmental alterations, interacting with genetic susceptibility factors [1], [3].

At the molecular level, melanoma is characterized by dysregulation of proliferative and survival pathways, particularly the mitogen-activated protein kinase (MAPK) and transforming growth factor beta (TGF-β) pathways [4], [5]. Activating mutations in the BRAF gene, especially BRAF V600E, drive constitutive MAPK activation in a substantial proportion of cases [6]. This discovery led to the development of targeted therapies such as vemurafenib (PLX4032), a selective BRAF inhibitor widely used in metastatic melanoma treatment [6]. The crystallographic structure of the BRAF–vemurafenib complex (PDB ID: 3OG7) provides a structural basis for structure-based drug design [7]. Although vemurafenib produces significant early clinical responses by suppressing MAPK signaling, therapeutic efficacy is frequently limited by acquired resistance and tumor adaptive mechanisms [8].

Natural products have gained increasing attention as potential complementary anticancer agents. Goji Berry (*Lycium barbarum*) contains bioactive compounds including polysaccharides, zeaxanthin, flavonoids, and anthocyanins with antioxidant and cytoprotective properties [9]. *Lycium barbarum* polysaccharides (LBPs) have demonstrated protective effects against UV-induced damage and modulation of oxidative stress pathways [10]. Fractionated neutral LBP (NLBP) exhibits pronounced immunomodulatory and antitumor activity, inhibiting melanoma growth by up to 66.7% in B16F10 models [11]. Zeaxanthin has shown selective inhibitory effects on melanoma cells through modulation of MAPK-related signaling [12]. Additionally, flavonoids and anthocyanins regulate redox balance, JNK, and FOXO pathways [10], [13], while LBPs also influence calcium, Hippo, and mTOR signaling, reducing oxidative stress and apoptosis.

Despite these biological findings, direct evaluation of the molecular interaction between *Lycium barbarum* bioactive compounds and key melanoma target, particularly BRAF, remains limited [12]. Systematic in silico molecular docking studies comparing these compounds with standard BRAF inhibitors such as vemurafenib are still lacking [6], and pharmacokinetic–toxicological profiling via ADMET prediction remains underexplored.

Therefore, this study aims to evaluate the anti-melanoma potential of Lycium barbarum bioactive compounds through molecular docking against the BRAF protein, using vemurafenib as a positive control. Unlike previous in silico studies, this research integrates comparative docking of 12 defined compounds, validated redocking (RMSD-based), ADMET profiling, and residue interaction similarity analysis with the native ligand, offering a more systematic and multi-parameter evaluation of potential BRAF inhibitors.

2. Methods

Study Design

This study was conducted using an in silico approach based on structure-based drug design (SBDD) to evaluate the potential interaction of bioactive compounds from

goji berry (Lycium barbarum) with the BRAF protein target involved in melanoma progression.

Software and Databases

The software used in this study included Discovery Studio Visualizer (BIOVIA, 2025), MGL Tools 1.5.6, AutoDock Tools 1.5.6, PyRx 0.8, and PyMOL 3.1.6.1. Molecular docking calculations were performed using AutoDock Vina, with PyRx serving as a graphical user interface (GUI) for ligand preparation and docking execution.

Materials and Databases

The materials used in this study include a three-dimensional (3D) structure of the target protein that plays a role in melanoma, namely the BRAF protein which is the most complex with PLX4032 ligand (PDB ID: 3OG7), which was obtained from the RCSB Protein Data Bank (https://www.rcsb.org/structure/3OG7) webserver. In addition, the compounds derived from goji berries (*Lycium barbarum)* used in this study are selected compounds whose entire chemical structure is presented in **Table 1**.

Table 1. Bioactive compounds identified from goji berry (*Lycium barbarum*) and used as test ligands in molecular docking analysis

Compound Name	PubChem ID	Source
Zeaxanthin	5280899	[14]
Myricetin	5281672	[15]
Quercetin	5280343	[16]
Ellagic acid	5281855	[17]
Galangin	5281616	[15]
Kaempferol	5280863	[17]
Chlorogenic acid	1794427	[17]
Hyoscyamine	23724783	[18]
Melatonin	896	[17]
Mono[5-methyl-2-(1-methylethyl)cyclohexyl]butanedioate	10199004	[19]
Tryptamine	1150	[20]
5-Methoxytryptamine	1833	[21]

Protein Preparation

The three-dimensional (3D) structure of the BRAF protein complexed with vemurafenib (PDB ID: 3OG7) was retrieved from the RCSB Protein Data Bank. The protein structure was prepared using AutoDock Tools by removing water molecules and other non-essential components, followed by the addition of polar hydrogen atoms. The prepared protein was then saved in PDBQT format [22].

The native ligand (vemurafenib) was separated from the protein complex and used as a positive control as well as for docking validation.

Ligand Selection and Preparation

The chemical structures of the ligands were obtained from the PubChem database and converted from SMILES format to PDB format using the Novopro online tool. The ligands were used in their default protonation states as provided by the database, without explicit tautomer enumeration. No additional geometry optimization was performed beyond standard preparation. Ligand preparation was then carried out using AutoDock Tools by assigning rotatable bonds via the torsion tree to ensure molecular flexibility. All ligands were saved in PDBQT format [22].

Docking Protocol Validation

Validation of the docking protocol was performed through a redocking approach of the native ligand (vemurafenib) into the active site of the BRAF protein using AutoDock Vina, with PyRx employed as a graphical user interface (GUI). The native ligand, which had been separated from the protein–ligand complex, was re-docked using the same parameters applied to the test compounds.

The accuracy of the docking protocol was evaluated based on the Root Mean Square Deviation (RMSD) between the docked ligand pose and the crystallographic ligand pose. RMSD calculation was performed using PyMOL by superimposing the docked structure onto the original complex. The docking protocol was considered valid if the RMSD value was ≤ 2.0 Å, indicating reliable reproduction of the native ligand binding pose. Lower RMSD values indicate higher accuracy of the docking method [23].

Molecular Docking Procedure

Molecular docking was carried out using AutoDock Vina through PyRx as a graphical user interface (GUI) for docking setup and execution. The prepared ligands and protein structures were imported into the Vina Wizard module in PyRx. The grid box was defined to encompass the active site of the BRAF protein based on the binding position of the native ligand (vemurafenib) obtained during validation. Docking simulations were performed with exhaustiveness set to 8, while other parameters, including the number of modes (9) and energy range (3 kcal/mol), were kept at their default values. Each docking simulation was performed once for each ligand. The resulting binding affinity values (kcal/mol) were analyzed to identify compounds with the strongest predicted binding interactions. The best docking poses were subsequently exported for further interaction analysis [24]

Interaction and Residue Similarity Analysis

The analysis of the ligand-protein interaction was carried out by visualizing the docking results using PyMOL. The docked protein and ligand files are combined to obtain a three-dimensional (3D) view that shows the position and orientation of the ligands on the active site of the protein. Furthermore, molecular interaction analysis was performed using Discovery Studio to identify the types of interactions formed, such as hydrogen bonds, hydrophobic interactions, and other interactions between ligands and amino acid residues on target proteins [22].

Binding affinity values (kcal/mol) obtained from molecular docking were used to evaluate ligand–protein interactions, where more negative values indicate stronger predicted binding. The binding affinities of the test ligands were compared with that of the native ligand (vemurafenib) as a reference to assess their relative binding strength. In addition, the similarity of amino acid residues (%) was calculated to evaluate the resemblance of ligand–protein interactions between test compounds and the native ligand. Residues were considered "shared" if identical amino acids were involved in interactions with both the test ligand and the native ligand, regardless of interaction type. Both hydrogen bond and hydrophobic interactions were treated equally. The similarity percentage was calculated by dividing the number of shared residues by the total number of interacting residues of the native ligand and multiplying by 100% [25]

ADMET and Drug-Likeness Prediction

Prediction of the pharmacokinetic and toxicological profile of the test compounds was carried out in silico using the ADMETLAB 3.0 webserver [26]. The parameters analyzed included absorption, distribution, metabolism, excretion, and potential toxicity (ADMET). In addition, a drug-likeness evaluation was also carried out based on Lipinski's Rule of Five, which included molecular weight (MW), lipophilicity

(LogP), number of hydrogen bond acceptors (nHA), and hydrogen bond donors (nHD), as initial criteria to predict the feasibility of compounds as oral drug candidates [27]. This comprehensive analysis aims to assess the pharmacokinetic potential, safety, and suitability of the compound as an anticancer drug candidate for melanoma skin before further experimental testing stages.

3. Results and Discussion

Docking Protocol Validation

Molecular docking is a computational method used to simulate the interaction between ligands and proteins in order to predict the position and orientation of ligands when binding to the target receptor [28]. The interaction results that are considered the best are those with the lowest bond energy value, because they show higher stability of the ligand–protein complex. However, before the bond affinity results are analyzed, a docking protocol validation is required to ensure that the method used is able to accurately reproduce the position of the native ligand.

Table 2. Grid box parameters and RMSD value obtained from docking protocol validation using vemurafenib as the native ligand

PDB ID	Size			Center			Spacing	RMSD
Code	X	Y	Z	X	Y	Z	Grid Point	
3OG7	24.9459	21.3716	21.3154	3.0279	-3.7369	-20.9459	0,357	0.956

Validation of docking protocols was carried out through a redocking approach using PyRx software on the active site of a protein known to bind to PLX4032 co-crystalline ligand (vemurafenib). The use of BRAF protein structures with the PDB code 3OG7 provides methodological advantages as these structures are available in complex form with BRAF selective inhibitors [7]. Presence of ligands *Native* (vemurafenib) allows for precise identification of the binding side as well as evaluation of the reliability of the docking protocol through the vemurafenib redocking process.

Binding Affinity and Interaction Profile of Lycium barbarum Bioactive Compounds

The grid box parameters applied in the redocking process are presented in **Table 2**, which includes the central coordinates (center X, Y, Z) as well as the grid dimensions (size X, Y, Z). The determination of the central coordinates is based on the geometric position of the co-crystalline ligand within the binding site, while the grid size is set to include all of the essential amino acid residues in the active site without excessively expanding the search space. The arrangement of this grid box aims to ensure that the ligand conformation search is focused on the biologically relevant active site [29].

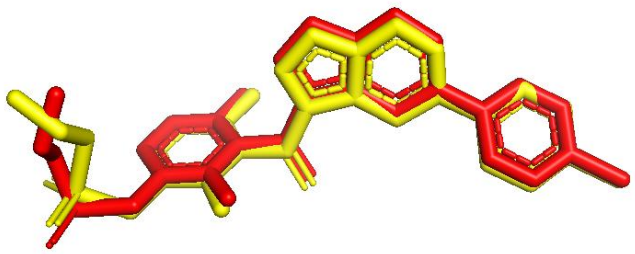

Figure 1. Overlay of the crystallographic pose of vemurafenib (red) and the redocked pose (yellow) in the BRAF protein (PDB ID: 3OG7).

The redocking results showed an RMSD value of 0.956 Å (< 2 Å), which indicates that the conformation of the docked ligands has a very small deviation compared to the crystal structure. RMSD values below 2 Å are generally accepted as an indicator that the docking protocol is capable of accurately reproducing the position of the original ligand [30]. In addition, **Figure 1** shows the result of the overlay (overlap) between the crystallographic ligand and the redocked ligand, where the two conformations appear to be squeezed together with minimal differences in atomic position. This visualization reinforces the quantitative results of the RMSD and confirms that the grid box parameters and docking settings used are appropriate to reliably predict the binding position of the ligand.

Table 3. Binding affinity values and amino acid residue interactions of *Lycium barbarum* bioactive compounds against the BRAF protein

Name Compounds	**Binding affinity**	**Amino Acid Residue Interactions**		**Similarity of Amino Acid Residues (%)**
		Hydrogen	Non Hydrogen	
Native (Vemurafenib)	-11,1	GLN A:530; ASP A:594; PHE A:595; GLY A:596	ILE A:463; ALA A:481; LYS A:483; LEU A:505; LEU A:514; THR A:529; TRP A:531; CYS A:532; PHE A:583	100
Zeaxanthin	-9,5	ASP A:594	VAL A:471; ALA A:481; LYS A:483; LEU A:514; TRP A:531; TYR A:538; HIS A:539; ALA A:543; PHE A:583	46,15
Myricetin	-9,2	ILE A:527; GLN A:530; CYS A:532	ILE A:463; VAL A:471; ALA A:481; LYS A:483; LEU A:514; TRP A:531; PHE A:583	61,53
Quercetin	-9,1	GLN A:530; CYS A:532	ILE A:463; VAL A:471; ALA A:481; LYS A:483; LEU A:514; TRP A:531; PHE A:583	61,53
Ellagic acid	-8,8	CYS A:532	VAL A:471; ALA A:481; TRP A:531; PHE A:583	30,76
Galangin	-8,7	GLN A:530; CYS A:532	ILE A:463; TRP A:531; PHE A:583; ALA A:481; VAL A:471; LEU A:514; LYS A:483	61,53
Kaempferol	-8,7	THR A:529; CYS A:532	ILE A:463; VAL A:471; ALA A:481; LYS A:483; LEU A:514; TRP A:531; PHE A:583	61,53
Chlorogenic acid	-8,2	THR A:529; ASN A:581; ASP A:594	VAL A:471; LYS A:483; PHE A:583	30,76
Hyoscyamine	-7,6	THR A:529	VAL A:471; LYS A:483; LEU A:505; ILE A:527	23,07
Melatonin	-7,4	CYS A:532	VAL A:471; ALA A:481; LYS A:483; LEU A:505; THR A:529; TRP A:531; CYS A:532	53,84
Mono[5-methyl-2-(1-methylethyl)cyclohexyl]butanedioate	-7,3	ALA A:481; THR A:529	VAL A:471; LEU A:514; CYS A:532; PHE A:583	38,46
Tryptamine	-6,3	ILE A:527	VAL A:471; ALA A:481; LEU A:514; CYS A:532; PHE A:583	30,76

5-Methoxytryptamine	-6,1	THR A:529, GLN A:530	PHE A:468; VAL A:471; ALA A:481; LEU A:514; CYS A:532; PHE A:583	46,15

The main parameter analyzed in the docking results is the binding affinity (ΔG) in kcal/mol units, which represents the Gibbs free energy estimate of the formation of protein–ligand complexes. Thermodynamically, a negative value of ΔG indicates that the binding process takes place spontaneously. The more negative the ΔG value, the greater the system's free energy decrease as the complex is formed, so the resulting complex is predicted to have higher stability [31], [32].

Lower (more negative) affinity values reflect the contribution of stronger intermolecular interactions between ligands and proteins, such as hydrogen bonds, hydrophobic interactions, van der Waals forces, as well as π–π or aromatic interactions. These combinations of interactions collectively play a role in stabilizing protein-ligand complexes. Therefore, in both comparative studies and virtual screening, compounds with more negative energy values are generally prioritized as potential candidates because they are assumed to have better binding strength.

Several previous studies have reported that binding affinity values of ≤ −8.0 kcal/mol are generally indicative of favorable ligand–protein interactions in in silico studies. For example, a study by Etana et al., [33] It is reported that phytochemical compounds with values greater than −8.0 kcal/mol exhibit strong interactions with target proteins, even in some cases having lower values than clinically approved drugs. In addition, research by [34]. explicitly states that the docking value of around −8 kcal/mol is included in the category *Good Binding Affinity* against the target protein. The findings reinforce that such energy ranges are generally thought to show stable and significant interactions in computational approaches.

Based on the results of docking between the active compounds of goji berries (*Lycium barbarum)* and the target protein of melanoma (**Table 3**), a range of binding affinity values was obtained indicating a potential interaction on the active site of the protein. Several compounds showed ≤ values of −8.0 kcal/mol, namely zeaxanthin (−9.5), myricetin (−9.2), quercetin (−9.1), ellagic acid (−8.8), galangin (−8.8), kaempferol (−8.7), and chlorogenic acid (−8.2). This value indicates that these compounds have a relatively good binding affinity based on criteria that have been reported in the literature.

In comparison, *the native* ligand (vemurafenib) showed an affinity value of −11.1 kcal/mol, which means it has the highest complex stability to the target protein. This shows that energetically, the compounds from goji berries (*Lycium barbarum)* have not exceeded the binding strength of *the native* ligand (vemurafenib). However, some compounds such as zeaxanthin, myricetin, and quercetin show relatively small energy differences compared to *native* (vemurafenib), so it can be said to have potential that is close to positive control.

Residue Similarity and Prioritization of Top Candidate Compounds

Visualization of docking results is carried out to observe and analyze the interaction pattern between ligands and amino acid residues at the binding site, both in the form of hydrogen bonds and hydrophobic interactions [35]. The similarity of interacting residues suggests that these compounds may occupy a binding region comparable to vemurafenib; however, this does not confirm an identical inhibitory mechanism. Interactions of active compounds Goji Berry (*Lycium Barbarum*) then

compared with the interaction pattern of vemurafenib with key residues at the BRAF V600E binding site. Similarity of interaction residues and competitive bond energy indicates the potential of the compound Goji Berry (*Lycium barbarum*) as an adjuvant candidate for melanoma therapy.

Table 4. Summary of key molecular interactions and prioritization rationale for the top candidate compounds

Compound	Binding Affinity (kcal/mol)	Shared Key Residues with Vemurafenib	Interaction Types	Rationale
Quercetin	-9.1	GLN530, CYS532, VAL471, ALA481, LYS483, LEU514, TRP531, PHE583	H-bond, hydrophobic	High similarity (61.53%) and stable interactions with key residues
Galangin	-8.7	GLN530, CYS532, VAL471, ALA481, LYS483, LEU514, TRP531, PHE583	H-bond, hydrophobic	Comparable residue interactions and good binding affinity
Myricetin	-9.2	GLN530, CYS532, VAL471, ALA481, LYS483, LEU514, TRP531, PHE583	H-bond, hydrophobic	Strong binding affinity but slightly different interaction pattern
Kaempferol	-8.7	CYS532, VAL471, ALA481, LYS483, LEU514, TRP531, PHE583	H-bond, hydrophobic	High residue similarity (61.53%) and stable interactions with key residues

To facilitate a clearer comparison of the most promising compounds, a summary of key interaction parameters is presented in **Table 4**. This highlights binding affinity, shared key residues with the native ligand (vemurafenib), and dominant interaction types. Among the tested compounds, quercetin and galangin exhibited favorable binding affinity along with a high percentage of residue similarity, indicating a binding pattern comparable to the native ligand. These compounds consistently interacted with key residues such as GLN A:530, CYS A:532, VAL A:471, ALA A:481, LYS A:483, LEU A:514, TRP A:531, and PHE A:583 through hydrogen bonds and hydrophobic interactions, supporting their potential as top candidate compounds. Although myricetin showed a slightly more negative binding affinity than quercetin, quercetin was prioritized because it combined strong binding affinity with high residue similarity and favorable interaction with key residues within the vemurafenib binding pocket.

Based on the visualization results in Table 4, the compounds myricetin, quercetin, galangin, and kaempferol show a greater number of interactions than zeaxanthin, ellagic acid, and chlorogenic acid, both in the form of hydrogen bonds and non-hydrogen interactions. This suggests that the four compounds have a wider involvement with important residues on the active site of the protein.

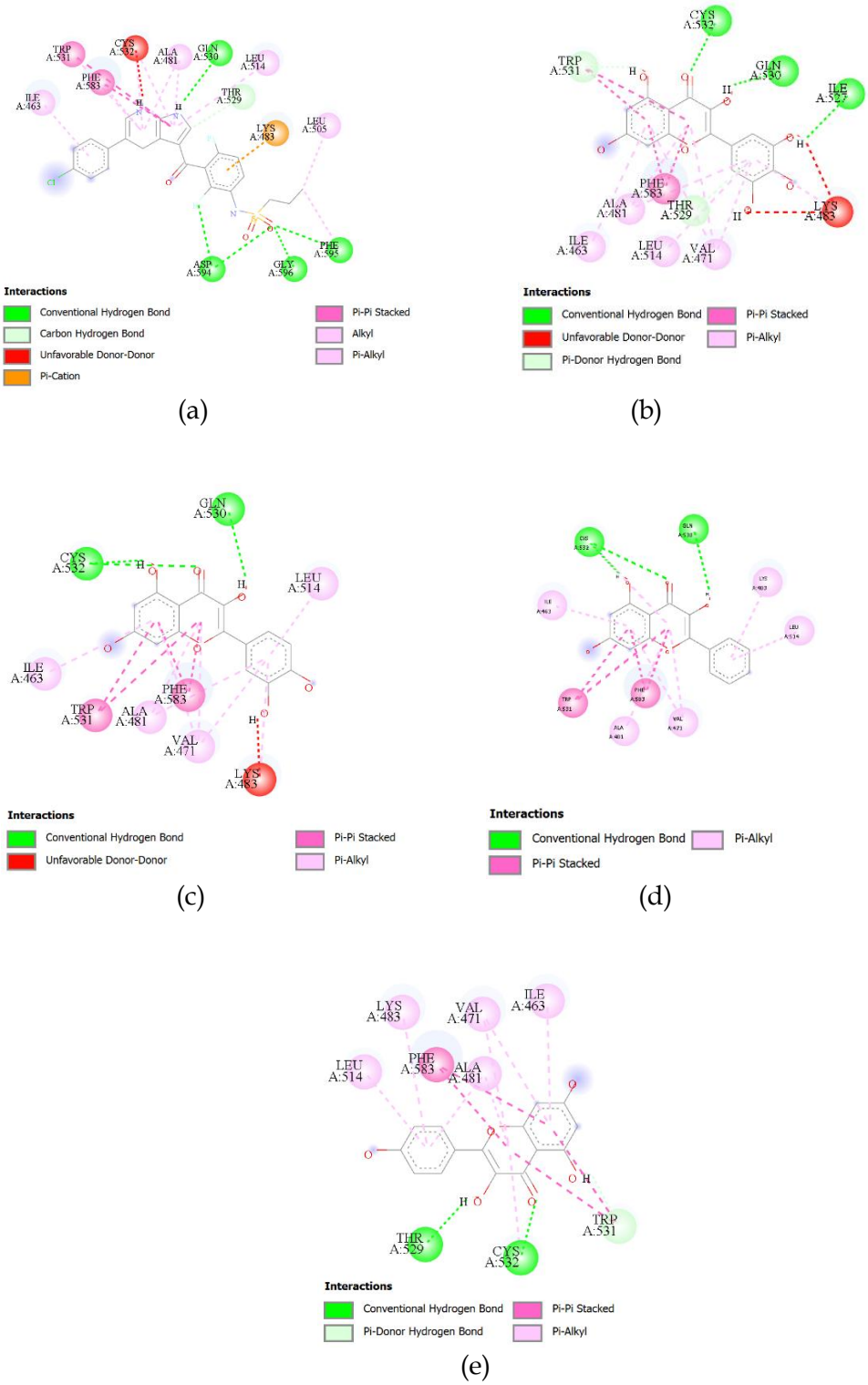

Figure 2. Redocking results in 2D (a) native ligands (vemurafenib), (b) myricetin, (c) quercetin, (d) galangin, (e) kaempferol.

According to Bollag *et al.*, [7], a residue directly involved in the bonding of hydrogen with a ligand *Native* (vemurafenib) GLN A:530; ASP A:594; PHE A:595 and GLY A:596. In addition, ligands *Native* (vemurafenib) also forms a non-hydrogen interaction with ILE A:463; ALA A:481; LYS A:483, LEU A:505; LEU A:514; THR A:529;

TRP A:531; CYS A:532 and PHE A:583 (**Figure 2a**). These residues can be considered the main components of active pouches because they are consistently involved in the formation of complexes with high stability. Therefore, the involvement of the same residue in the test compound is an important indicator that plays a role in orienting the ligand appropriately in the binding pocket so as to increase the beneficial interaction [25].

Myricetin (**Figure 2b**) forms a hydrogen bond with ILE A:527; GLN A:530; CYS A:532. In addition, non-hydrogen interactions are formed with ILE A:463; VAL A:471; ALA A:481; LYS A:483; LEU A:514; TRP A:531 and PHE A:583. The involvement of Gln530 and Cys532—which are in the active site environment and the retention of important hydrophobic residues—show a fairly high resemblance to *the interaction* pattern with native (vemurafenib). This is reflected in the residue similarity percentage of 61.53%, indicating that more than half of the key residues interacting with the native ligand were also involved in the myricetin–BRAF complex.Quercetin (**Figure 2c**) shows a pattern very similar to myricetin. Hydrogen bonds are formed with GLN A:530 and CYS A:532, while non-hydrogen interactions involve ILE A:463; VAL A:471; ALA A:481; LYS A:483; LEU A:514; TRP A:531 and PHE A:583. A residue similarity of 61.53% indicates that more than half of the key residues interacting with the native ligand (vemurafenib) were also involved in the quercetin–BRAF complex, suggesting that quercetin may occupy a comparable binding region within the BRAF active site.

Galangin (**Figure 2d**) shows the widest interaction pattern among all test compounds. Hydrogen bonds are formed with GLN A:530 and CYS A:532, which include several important residues that also appear in native ligands (vemurafenib). Non-hydrogen interactions occur with ILE A:463; TRP A: 531; PHE A:583; ALA A:481; VAL A:471; LEU A:514; LYS A:483. The percentage of residue similarity (61.53%) showed a good similarity of binding modes. The hydrogen bonds formed have the potential to improve the stability of the complex through the contribution of stronger electrostatic and polar interactions.

Kaempferol forms hydrogen bonds with THR A:529 and CYS A:532, and maintains non-hydrogen interactions with ILE A:463; VAL A:471; ALA A:481; LYS A:483; LEU A:514; TRP A:531 and PHE A:583. With a residue similarity percentage of 61.53%, this compound exhibits a fairly stable interaction pattern and still retains most of the important residues on the active site.

Overall, the involvement of key residues such as GLN A:530; ASP A:594; CYS A:532; LYS A:483; LEU A:514; TRP A:531; and PHE A:583 showed that these compounds were able to occupy the same active pockets as native ligands (vemurafenib). The more important residues are preserved, especially through the combination of hydrogen bonds and hydrophobic interactions, the more likely it is that a stable complex will form and potentially have an inhibitory effect on the target protein.

Drug-Likeness and ADMET Prediction

In line with the molecular docking results, the assessment of drug compound candidates is based not only on the strength of the interaction against the target, but also on its pharmacokinetic and pharmacodynamic characteristics. This evaluation is generally carried out through the prediction of ADMET parameters (*absorption, distribution, metabolism, excretion, and toxicity*) which is an approach *in silico* It is important in the early stages of drug development to predict the pharmacokinetic behavior and safety of a compound before testing *in vivo*. Computing-based prediction methods such as ADMETLAB 3.0 have been widely used to evaluate natural compounds, including

flavonoids, because they are able to provide a preliminary picture of absorption, distribution, metabolism, excretion, and toxicity quickly and efficiently [36].

In addition to ADMET analysis, drug-likeness evaluation was performed using Lipinski's Rule of Five (RO5) to predict the potential oral bioavailability of a compound. This rule is based on four main parameters, namely molecular weight (MW < 500 Da), lipophilicity (logP < 5), the number of hydrogen bond acceptors (nHA < 10), and the number of hydrogen bond donors (nHD < 5). Compounds that violate more than one RO5 criterion generally have a higher risk of poor intestinal absorption and limited membrane permeability, making them less ideal for development as an oral drug [37], [38].

Table 5. Drug-likeness evaluation of selected candidate compounds based on Lipinski's Rule of Five

No	Compounds	Lipinski Rule of Five			
		MW	**LogP**	**nHA**	**nHD**
1	Myricetin	318.04	1.115	8.0	6.0
2	Quercetin	302.04	-3.722	7.0	5.0
3	Galangin	270.05	2.225	5.0	3.0
4	Kaempferol	286,05	1,965	6.0	4.0

Based on the data in the **Table 5**, all test compounds had a molecular weight below 500 Da and a log P value of less than 5, indicating that their molecular size and lipophilicity level were still within the range that supported passive diffusion through the biological membrane. Quercetin, galangin, and kaempferol met all RO5 criteria without violation, with an nHA value of no more than 10 and an nHD of less than 5 indicating the most optimal drug-likeness profile for potential oral administration.

In contrast, myricetin showed one violation of RO5 on the total parameter of the hydrogen bond donor (nHD > 5). This reflects the high polarity of the molecules due to the large number of hydroxyl groups, which has the potential to decrease membrane permeability and oral absorption. However, based on the current literature, a single violation of the RO5 criteria is still tolerable, especially in natural compounds with strong biological activity, as long as it is supported by a safe ADME profile and toxicity [39].

Table 6. Predicted ADMET profiles of selected goji berry (*Lycium barbarum*) bioactive compounds using ADMETlab 3.0

Compounds	Absorption	Distribution			Metabolism				Excretion		Toxicity	
	HIA (%)	Caco 2	PPB (%)	BBB (%)	CYP2C19	CYP2C9	CYP2D6	CYP3A4	CL	T1/2	Mutagen	Carcinogens
Myricetin	-	-6.454	97	---	---	+++	---	+++	6,775	1.629	0,657	0.502
Quercetin	--	-6,177	98,7	---	---	-	---	---	8.289	1.586	0.586	0.6
Galangin	---	-5,353	98,2	---	-	+++	---	--	4,635	1,052	0.560	0.706
Kaempferol	---	-5.969	97,9	---	---	++	---	+++	5.694	1.388	0.546	0.716

Note: The symbols indicate relative prediction levels from ADMETlab 3.0:
--- = very low, -- = low, - = slightly low, + = slightly high, ++ = high, and +++ = very high predicted probability.
HIA, human intestinal absorption; PPB, plasma protein binding; BBB, blood–brain barrier; CYP, cytochrome P450; CL, clearance; T1/2, half-life.

The results of the ADMET prediction show that myricetin, quercetin, galangin, and kaempferol have different pharmacokinetic profiles, especially in the parameters of absorption, distribution, metabolism, and excretion (**Table 5**). In the absorption aspect, all compounds showed low Caco-2 permeability values, which indicates the limitation of passive diffusion through the intestinal epithelium. Myricetin and quercetin showed relatively better absorption than galangin and kaempferol, although they were generally still relatively low. This low absorption is closely related to the high polarity of the molecules as well as the abundance of hydroxyl groups in the flavonoid structure, which can inhibit the penetration of lipid membranes. These findings are in line with previous reports that flavonoids such as quercetin have low oral bioavailability due to limited intestinal permeability [37].

In terms of distribution, myricetin, quercetin, galangin, and kaempferol exhibit very high plasma protein bonds (>97%), which indicates that most of the compounds are in bound form within the systemic circulation. High plasma protein bonds have the potential to extend the residence time of compounds in plasma, but may decrease the free fraction available to interact with biological targets. The entire compound is also predicted to be unable to penetrate the cerebral blood barrier (BBB), which is a beneficial characteristic for anticancer drug candidates because it can minimize potential side effects on the central nervous system. These distribution characteristics are consistent with reports that flavonoids generally have a high affinity for plasma proteins and limited BBB penetration.

In terms of metabolism, galangin, myricetin, and kaempferol are predicted to potentially inhibit several cytochrome P450 isoenzymes, especially CYP2D6 and CYP3A4, indicating a potential drug-drug interaction when used systemically. In contrast, quercetin exhibits a more moderate metabolic profile with more limited interactions of CYP enzymes. These results are in line with in silico and experimental studies that report that quercetin and its derivatives can interact with key CYP enzymes, but are still within pharmacological safety limits [37].

At the excretory parameters, quercetin shows the highest clearance value, which signifies relatively rapid elimination from the body. In contrast, galangin and kaempferol exhibit lower clearance values, with a relatively longer half-life, thus potentially maintaining systemic exposure for a more stable duration despite limited absorption.

In terms of toxicity, all compounds show low mutagenic and carcinogenic potential. This safety profile supports the potential use of these compounds as anticancer candidates, particularly natural flavonoids which are generally reported to have high safety margins and rarely cause significant systemic toxicity [37]. Thus, although quercetin and galangin have limitations in oral absorption and potential metabolic interactions, their favorable distribution profile, moderate excretion parameters, and relatively low predicted toxicity support their potential for further development. Formulation strategies that improve bioavailability may be required to enhance their therapeutic applicability. In addition, their high residue similarity with vemurafenib suggests that these compounds may occupy a comparable binding region within the BRAF active site.

Study Limitations and Future Validation

The present in silico study demonstrated that quercetin and galangin are the most promising bioactive compounds from Lycium barbarum based on complementary evaluation criteria. Quercetin showed strong predicted binding affinity toward the

BRAF target and conserved key amino acid interactions comparable to vemurafenib, whereas galangin exhibited the most favorable drug-likeness and ADMET profile. These findings suggest that both compounds may serve as preliminary candidates for further development as BRAF-targeting adjuvant agents in melanoma therapy. However, because the results are based on computational prediction, further validation through molecular dynamics simulations, BRAF kinase inhibition assays, melanoma cell-based assays, and in vivo studies is required to confirm their biological activity, safety, and therapeutic relevance.

4. Conclusion

The docking results demonstrated that quercetin and galangin exhibited strong binding affinities toward the BRAF protein, with binding energy values of −9.1 kcal/mol and −8.8 kcal/mol, respectively, while maintaining interactions with key amino acid residues within the BRAF active site similar to those observed for the native ligand. The percentage of shared interacting residues relative to vemurafenib was recorded at 61.5%, suggesting favorable interaction similarity and potential stability of the ligand–protein complexes. ADMET analysis indicated that galangin possessed the most balanced pharmacokinetic profile, whereas quercetin displayed the lowest binding energy, suggesting a potentially stronger interaction with the BRAF V600E receptor compared to the other tested compounds. Collectively, these findings indicate that both compounds have promising predicted potential for further development as adjuvant candidates in melanoma therapy. However, these results are based on computational predictions and require further validation through experimental studies, such as in vitro BRAF kinase assays and melanoma cell-based assays.

Acknowledgements:

The authors would like to thank the Department of Pharmaceutical Chemistry, Faculty of Pharmacy, Universitas Islam Sultan Agung, Semarang, Indonesia, for providing academic support during the preparation of this study.

Conflicts of Interest:

The authors declare no conflict of interest regarding the publication of this paper.

References

[1] E. Montuori, A. Capalbo, and C. Lauritano, "Marine compounds for melanoma treatment and prevention," *Int. J. Mol. Sci.*, vol. 23, no. 18, art. no. 10284, 2022. [Online]. Available: https://doi.org/10.3390/ijms231810284

[2] H. Bokharaie and W. Kolch, "Analysis of alternative mRNA splicing in vemurafenib-resistant melanoma cells," *Biomolecules*, vol. 12, no. 7, art. no. 993, 2022. [Online]. Available: https://doi.org/10.3390/biom12070993

[3] N. Dubbini *et al.*, "Melanoma prevention: Comparison of different screening methods for the selection of a high risk population," *Int. J. Environ. Res. Public Health*, vol. 18, no. 4, art. no. 1953, 2021. [Online]. Available: https://doi.org/10.3390/ijerph18041953

[4] Y. Ke and X. Wang, "TGFβ signaling in photoaging and UV-induced skin cancer," *J. Invest. Dermatol.*, vol. 141, pp. 1104–1110, 2021/2022. [Online]. Available: https://doi.org/10.1016/j.jid.2020.11.007

[5] M. Manganelli *et al.*, "Skin photodamage and melanomagenesis: A comprehensive review," *Cancers*, vol. 17, no. 11, art. no. 1784, 2025. [Online]. Available: https://doi.org/10.3390/cancers17111784

[6] B. Aires-Lopes *et al.*, "Violacein improves vemurafenib response in melanoma spheroids," *Nat. Prod. Res.*, vol. 38, no. 19, pp. 3417–3420, 2024. [Online]. Available: https://doi.org/10.1080/14786419.2023.2244134

[7] G. Bollag *et al.*, "Clinical efficacy of a RAF inhibitor needs broad target blockade in BRAF-mutant melanoma," *Nature*, vol. 467, pp. 596–599, 2010/2011. [Online]. Available: https://doi.org/10.1038/nature09454

[8] M. Radi, "Characterization of vemurafenib-resistant melanoma cell lines reveals novel hallmarks of targeted therapy resistance," *Int. J. Mol. Sci.*, vol. 23, no. 17, art. no. 9910, 2022. [Online]. Available: https://doi.org/10.3390/ijms23179910

[9] F. Teixeira, A. M. Silva, C. Delerue-Matos, and F. Rodrigues, "*Lycium barbarum* berries (Solanaceae) as source of bioactive compounds for healthy purposes: A review," *Int. J. Mol. Sci.*, vol. 24, no. 5, art. no. 4777, 2023. [Online]. Available: https://doi.org/10.3390/ijms24054777

[10] J. Liu *et al.*, "*Lycium barbarum* polysaccharides inhibit ischemia/reperfusion-induced myocardial injury via the Nrf2 antioxidant pathway," *Toxicol. Rep.*, vol. 8, pp. 657–667, 2021. [Online]. Available: https://doi.org/10.1016/j.toxrep.2021.03.019

[11] J.-L. Duan *et al.*, "Comparative study on physicochemical characterization and immunomodulatory activities of neutral and acidic *Lycium barbarum* polysaccharides," *Biomed. Pharmacother.*, vol. 181, art. no. 117659, 2024. [Online]. Available: https://doi.org/10.1016/j.biopha.2024.117659

[12] A. Bunea *et al.*, "Zeaxanthin-rich extract from superfood *Lycium barbarum* selectively modulates the cellular adhesion and MAPK signaling in melanoma versus normal skin cells in vitro," *Molecules*, vol. 26, no. 2, art. no. 333, 2021. [Online]. Available: https://doi.org/10.3390/molecules26020333

[13] Y. Niu, J. Liao, H. Zhou, C. Wang, L. Wang, and Y. Fan, "Flavonoids from *Lycium barbarum* leaves exhibit anti-aging effects through redox-modulation," *Molecules*, vol. 27, no. 15, art. no. 4952, 2022. [Online]. Available: https://doi.org/10.3390/molecules27154952

[14] KNApSAcK Family Database, "KNApSAcK Core Database: Zeaxanthin," 2025. [Online]. Available: https://www.knapsackfamily.com/knapsack_core/result.php?sname=all&word=ZEAXANTHIN

[15] X. Qiang *et al.*, "Deep-processing fermentation products," 2023. [Online]. Available: https://www.mdpi.com/1420-3049/28/24/8044

[16] X. Qiang *et al.*, "Bioactive components of *Lycium barbarum* and deep-processing fermentation products," *Molecules*, vol. 28, no. 24, art. no. 8044, 2023. [Online]. Available: https://doi.org/10.3390/molecules28248044

[17] H. Kantar and N. E. Bayram, "Sustainable optimization of ohmic heating–assisted extraction of polyphenolics from goji berry (*Lycium barbarum* L.): LC–MS/MS profiling and blueness–greenness assessment," *Food Anal. Methods*, vol. 18, pp. 1884–1898, 2025. [Online]. Available: https://doi.org/10.1007/s12161-025-02831-w

[18] KNApSAcK Family Database, "KNApSAcK Core Database: Hyoscyamine," 2025. [Online]. Available: https://www.knapsackfamily.com/knapsack_core/top.php

[19] KNApSAcK Family Database, "KNApSAcK Core Database: Mono[5-methyl-2-(1-methylethyl)cyclohexyl] butanedioate," 2025. [Online]. Available: https://www.knapsackfamily.com/knapsack_core/top.php

[20] KNApSAcK Family Database, "KNApSAcK Core Database: Tryptamine," 2025.

[Online]. Available: https://www.knapsackfamily.com/knapsack_core/top.php
[21] KNApSAcK Family Database, "KNApSAcK Core Database: 5-Methoxytryptamine," 2025. [Online]. Available: https://www.knapsackfamily.com/knapsack_core/information.php?word=C00051985
[22] N. Frimayanti, M. Djohari, and A. N. Khusnah, "Molecular docking of chalcone analogue compounds as inhibitors for lung cancer A549 cells," *J. Ilmu Kefarmasian Indones.*, vol. 19, no. 1, pp. 87–95, 2021. [Online]. Available: https://doi.org/10.35814/jifi.v19i1.765
[23] F. M. Fauzi, Y. U. Wutsqa, and N. A. Rohmatika, "Bioavailability and molecular docking study of phenolic compounds of *Ocimum sanctum* L. as estrogen receptor-α inhibitors in breast cancer cells," 2024. [Online]. Available: https://doi.org/10.37089/jofar.vi0.297
[24] A. B. Pratama, R. Herowati, and H. M. Ansory, "Molecular docking study of nutmeg essential oil compounds (*Myristica fragrans* H.) and myristicin derivatives toward skin cancer therapeutic targets," *Maj. Farm.*, vol. 17, no. 2, p. 233, 2021. [Online]. Available: https://doi.org/10.22146/farmaseutik.v17i2.59297
[25] A. Rahmadani, C. N. Putri, and A. K. Wachidah, "In silico evaluation of tamarind leaf flavonoids targeting ERα as anti-breast cancer agents using molecular docking," *Indonesian J. Pharm. Educ.*, vol. 5, no. 3, pp. 343–356, 2025. [Online]. Available: https://doi.org/10.37311/ijpe.v5i3.33673
[26] L. Fu *et al.*, "ADMETlab 3.0: An updated comprehensive online ADMET prediction platform enhanced with broader coverage, improved performance, API functionality and decision support," *Nucleic Acids Res.*, vol. 52, pp. 422–431, 2024. [Online]. Available: https://doi.org/10.1093/nar/gkae236
[27] S. Nhlapho and I. Munien, "Druggability of pharmaceutical compounds using Lipinski rules with machine learning," 2024. [Online]. Available: https://etflin.com/file/document/20260310033647_622338_dbf1c3c0.pdf
[28] E. G. Clarensia *et al.*, "In silico study of mangiferin derivatives from mango as inhibition of protein tyrosine phosphatase 1B," *J. Silico Vitr. Pharmacol.*, vol. 22, no. 2, 2025. [Online]. Available: https://doi.org/10.21767/2469-6692.10024
[29] R. Hasan and R. Herowati, "Molecular docking and pharmacokinetic studies of *Moringa oleifera* as angiotensin-converting enzyme inhibitors," 2024. [Online]. Available: https://doi.org/10.20473/jfiki.v11i12024.80-88
[30] R. Ruswanto, R. Mardianingrum, and D. Kesuma, "Design, molecular docking, and molecular dynamics of thiourea–iron(III) metal complexes as NUDT5 inhibitors for breast cancer treatment," *Heliyon*, vol. 8, 2022. [Online]. Available: https://doi.org/10.1016/j.heliyon.2022.e10694
[31] A. T. Perdana *et al.*, "Molecular docking of potential anti-COVID-19 compounds (RCSB PDB) using PyMOL," 2021. [Online]. Available: https://doi.org/10.31000/jika.v5i2.4516
[32] A. G. Riwu *et al.*, "Molecular docking analysis of anti-dengue activity of *Moringa oleifera* leaves bioactive compounds," *Cendana Med. J.*, vol. 12, no. 2, pp. 1–14, 2024. [Online]. Available: https://doi.org/10.35508/cmj.v12i2.23665
[33] L. Etana *et al.*, "Combining empirical knowledge, in silico molecular docking and ADMET profiling to identify therapeutic phytochemicals from *Brucea antidysentrica* for acute myeloid leukemia," *PLOS ONE*, vol. 17, p. e0270050, 2022. [Online]. Available: https://doi.org/10.1371/journal.pone.0270050
[34] Y. El Bakri *et al.*, "Synthesis and identification of novel potential molecules against

COVID-19 main protease through structure-guided virtual screening approach," *Appl. Biochem. Biotechnol.*, pp. 3602–3623, 2021. [Online]. Available: https://doi.org/10.1007/s12010-021-03615-8

[35] D. Suriyeni, Z. Mukarromah, and M. R. Ridho, "Exploration of molecular docking of *Orthosiphon stamineus* flavonoids against cyclooxygenase (COX) as anti-inflammatory agents," *Blantika Multidiscip. J.*, vol. 2, no. 8, pp. 782–789, 2024. [Online]. Available: https://doi.org/10.57096/blantika.v2i8.191

[36] A. A. Nugroho, M. S. Hadi, C. Adianto, J. Akbar, and K. Putra, "Molecular docking and ADMET prediction studies of flavonoids as multi-target agents in COVID-19 therapy: Anti-inflammatory and antiviral approaches," vol. 34, no. 4, pp. 651–664, 2023. [Online]. Available: https://doi.org/10.22146/ijp.4126

[37] A. Caminero *et al.*, "Absorption matters: A closer look at popular oral bioavailability rules for drug approvals," 2023. [Online]. Available: https://doi.org/10.1002/minf.20230011

[38] G. Miebs and A. Mielniczuk, "Beyond the arbitrariness of drug-likeness rules: Rough set theory and decision rules in the service of drug design," 2024. [Online]. Available: https://doi.org/10.3390/app14219966

[39] C. V. Simoben, S. B. Babiaka, C. T. Namba-Nzanguim, and B. Eni, "Challenges in natural product-based drug discovery assisted with in silico-based methods," *RSC Adv.*, vol. 13, pp. 31578–31594, 2023. [Online]. Available: https://doi.org/10.1039/D3RA06831E